FUDMA Journal of Engineering and Technology
ISSN: 3092-9385
https://fjet.fudutsinma.edu.ng/index.php/fjet/
Volume 2, Issue 2, 2026, 29-44

Development and Performance Evaluation of an Injection Moulding Machine for Recycled Polymer Composite Production

Adefemi O. ADEODU[1*], Banjo C. ADEDOKUN[2], Amos A. ADEGBITE[3]

[1*,2,3]Department of Project Management, Bells University of Technology, Ota, Ogun State, Nigeria
[2,3]Department of Mechanical Engineering, Afe Babalola University, Ado-Ekiti, Ekiti State, Nigeria

[1*]aoadeodu@bellsuniversity.edu.ng, [2]bjadedokun@gmail.com, [3]aaadegbite@bellsuniversity.edu.ng

Abstract

The increasing demand for cost-effective polymer composite products with improved dimensional stability, mechanical properties, and surface quality has necessitated the optimization of injection moulding process parameters. However, inadequate control of injection pressure and injection time often results in poor mould cavity pressure distribution, leading to defects and inferior mechanical performance. This study investigated the effects of injection pressure and injection time on the mould cavity pressure of low-density polyethylene (LDPE) reinforced with aluminium powder and carbon black powders processed at 250°C and 200°C, respectively. Specifically, the study aimed to evaluate the influence of injection pressure and injection time on cavity pressure and establish their implications for product quality. An experimental research design was adopted using a locally fabricated injection moulding machine with a maximum injection pressure of 2,500 bar, a cylinder diameter of 22 mm, and a product capacity of 200 g. LDPE/aluminium and LDPE/carbon black composites were moulded under varying injection pressures and injection times, and cavity pressures were measured and analysed. The results showed a direct relationship between injection pressure and mould cavity pressure. For LDPE/aluminium, cavity pressure increased from 22 MPa to 42 MPa as injection pressure increased from 39 MPa to 70 MPa, while LDPE/carbon black recorded an increase from 20 MPa to 37 MPa under similar conditions. Conversely, increasing injection time reduced cavity pressure from 47 MPa to 30 MPa for LDPE/aluminium and from 39 MPa to 30 MPa for LDPE/carbon black. The study concludes that higher injection pressures and shorter injection times produce superior mould cavity pressures, resulting in improved dimensional stability, enhanced mechanical properties, and better surface appearance of moulded products. The study contributes empirical data for optimizing injection moulding parameters and provides a basis for improving the processing of reinforced LDPE composites.

Keywords: *Composites, Cyclic manufacturing, defects, Injection moulding, Polymer.*

1.0 Introduction

Injection moulding is an intermittent cyclic manufacturing process in which molten polymer is injected into a mould cavity to produce components with high dimensional accuracy, excellent surface finish and complex geometries [1]. Owing to its high production efficiency, short cycle times, repeatability and cost-effectiveness, injection moulding has become one of the most widely adopted manufacturing processes for producing plastic products used in domestic, commercial, automotive, medical, electrical and industrial applications [1-2]. Because the plastic material, part geometry, mould structure and process circumstances all affect the quality of parts made by injection moulding [3–4], it is crucial to effectively regulate the influencing factors during the moulding process [5–8]. Filling is the first step in a conventional injection moulding process, in which the molten polymer is pushed into a hollow whose wall is kept at a temperature low enough to cause solidification. Packing, which takes into consideration shrinkage during solidification when the cavity is full, comes next. Holding follows packing to improve the product's dimensional stability under extremely high pressure. The last phase, known as cooling, involves letting the material cool inside the chamber until it is safe to be expelled without causing structural damage [9]. The literature claims that the filling step is the most thoroughly researched because of mouldability and the filling stage is crucial to thermoplastic and thermoset process optimization. Furthermore, in the case of injection moulding of reinforced polymer, the orientation assumed by the polymer in the different sections of the parts depends entirely on the flow pattern in the cavity during filling and, to a lesser extent, on the outcome of subsequent orientation during packing [10]. Injection moulding is governed by complex melt flow phenomena during cavity filling, including shear flow across the cavity thickness, convective flow along the cavity geometry and fountain flow at the advancing melt front [11]. These flow characteristics influence the distribution and packing of reinforcing particles within the polymer matrix and consequently affect the quality of the moulded component [12]. Among the geometric parameters, the gating system plays a crucial role because it controls the manner in which the molten composite enters the mould cavity, thereby influencing melt flow behaviour, pressure distribution and particle dispersion [13]. The cavity pressure profile and its reproducibility significantly affect the mass, dimensional stability, mechanical performance and surface quality of injection-moulded products [14]. For particulate-reinforced polymer composites, the mechanical and physical properties of the final product depend

Received: 22/06/2026; Revised: 04/07/2026; Accepted: 08/07/2026; Published: 11/07/2026

largely on the type, size, morphology and concentration of the reinforcing particles, as well as the quality of particle dispersion and the interfacial adhesion between the particles and the polymer matrix [15]. Poor particle distribution or inadequate packing during mould filling may result in particle agglomeration, void formation and non-uniform shrinkage, which adversely affect the dimensional accuracy and mechanical integrity of the moulded component [16]. Processing conditions such as injection pressure, injection temperature, injection time and holding pressure have a considerable influence on melt flow behaviour, cavity pressure evolution, particle distribution and the consolidation of the composite material [17]. Among these processing parameters, injection pressure and injection time are particularly important because they directly determine the cavity pressure developed during mould filling and packing. Higher injection pressures generally enhance mould filling, improve particle packing, reduce void formation and promote better interfacial bonding between the LDPE matrix and reinforcing particles [18]. Longer injection times may reduce cavity pressure due to slower filling rates and increased heat loss, potentially leading to inadequate packing, greater shrinkage and reduced product quality [17-18]. Several studies have demonstrated that cavity pressure is one of the most reliable indicators of process stability and product quality because it reflects the effectiveness of melt filling and packing during injection moulding [19]. Previous computational and experimental investigations have shown that increasing the injection flow rate generally results in higher mould cavity pressures [15-16], whereas lower flow rates produce reduced cavity pressures and less effective material compaction [20]. Although earlier studies primarily focused on fibre-reinforced polymer composites, similar flow dynamics govern particulate-filled systems, where cavity pressure influences particle distribution, packing density and overall composite quality [21-22]. However, compared with fibre-reinforced polymers, there is relatively limited information regarding the combined effects of injection pressure and injection time on mould cavity pressure and the resulting quality characteristics of particulate-reinforced low-density polyethylene (LDPE) composites, particularly those reinforced with aluminium and carbon black powders. This study investigates the influence of these processing parameters on mould cavity pressure to establish their implications for the dimensional stability, mechanical properties and surface quality of injection-moulded LDPE particulate composites. One of the important processing parameters that has been discussed in a number of studies is injection moulding pressure. Zhang et al. [23] shown that if the mould's temperature is sufficiently low, the cavity pressure will progressively decrease and eventually disappear. As the cavity pressure rises, a number of material properties alter. They discovered that the cavity pressure increases with the holding pressure. The temperature of the mould affects the cavity pressure, which rises as the mould's temperature rises. Wen-Cheng et al. [24] investigated how injection pressure and holding time affected injection moulded parts' dimensions, surface fatness, green density, and sintering density. The findings show that the trend of the property changes under these pressures is shown by the pressure–time traces where the gate pressure is raised from 22 to 117 MPa and the holding period up to 75 seconds. To improve the moulded dimension and reduce the surface sinking of green pieces, high holding pressures and longer holding times would be preferred. The statistics demonstrate that the bulk density of green pieces is not significantly affected by holding time or pressure. Analysis of a similar experiment on polycarbonate material by Pareek and Bhamniya [25] reveals a direct correlation between the material's tensile strength and process variables like melting temperature and injection pressure. Hassan [26], who conducted an experiment on the impact of injection moulding settings on the polymer pressure inside the mould cavity and the final product weight, was another contributor to this study. Numerous processing parameters, including packing pressure, packing duration, injection pressure, time and temperature, were taken into consideration. The work is restricted to a homogenous mixture of low-density polyethylene (LDPE) and polystyrene (PS). Using Taguchi's orthogonal array, Singh et al. [2] conducted an experiment to find out how injection process parameters affected tensile strength. The investigation was restricted to a single homogenous material, polypropylene (PP), and determined the ideal process parameters to assess the product's quality solely in terms of strength. Wu et al. investigated the impact of microscopic features on the shrinkage of macroscopic products [27]. The in-plane shrinkage was measured using the optical technique on flat specimens with and without microstructures. The impact of injection and packing pressures on the electrical and microstructural characteristics of a carbon black-filled polymer composite was also examined by Wu et al. [27]. The authors laid the groundwork for improving the final products' mechanical and aesthetic qualities. It is still possible to look at other quality metrics, such as dimensional stability. This work's originality stems from the extensive body of literature that has been produced from the ground-breaking experimental work and the application of computational tools that concentrate on short fibre-polymer. There is virtually little research on how injection parameters affect particle reinforced polymer orientation. In order to determine the final product's quality in terms of dimensional stability, mechanical properties, and appearance, this work examined the effects of injection pressure and time on the mould cavity pressure of low-density polyethylene (LDPE) mixed with aluminium and low-density polyethylene (LDPE) mixed with carbon black powders at 250 ^{o}C and 200 ^{o}C injection temperatures, respectively.

Received: 22/06/2026; Revised: 04/07/2026; Accepted: 08/07/2026; Published: 11/07/2026

2.0 Materials and Method

The materials employed in the study are low density polyethylene (LDPE) mixed with aluminium (pyro powder) and carbon black (thermal black) powder separately. The LDPE was supplied by General Polymer Thermoplastic Materials, LLC, Auburn Hills, MI while the aluminium and carbon black powder were supplied by Haojian Chemical Technology Co. Ltd, China. Tables 1-3 show the properties of LDPE, aluminium and carbon black powder respectively. The injection moulding machine was locally developed in the Engineering Workshop of Afe Babalola University, Ado-Ekiti, Nigeria. The polymer composites pellets are produced by mixing 25 % weight fraction of aluminium and carbon black powder separately with 150 grams of Low-Density Polyethylene (LDPE) to make 200 grams of each polymer composite. The mixing was carried out with a mixer (ME100LA) at a temperature of 190^{o}C for 20 minutes at a speed of 200 rpm. After the mixing, the mixtures were then passed into a twin-screw plastic pelletizer, and later fed into the injection moulding machine.

Table 1: Properties of LDPE

S/N	Property	Description
1	Density range (g/cm$^{3)}$	0.91- 0.94
2	Tensile Strength (N/mm^{2})	10 – 20
3	Impact Strength	No Break
4	Thermal Co-efficient of expansion (K^{-1})	100-220 x10^{-6}
5	Max used Temperature (^{o}C)	250
6	Melting Point (^{o}C)	110
7	Glass Transition Temperature (^{o}C)	-125
8	MFI	190°C/2.16kg

Table 2: Properties and composition of aluminium powder

S/N	Property	Description
1	Shape	Spherical, irregular, or flake (atomized powders are predominantly spherical or irregular
2	Composition	Aluminium (Al): 99.0–99.9 wt%; trace impurities (Si, Fe, Cu, Mg, Zn, Mn) <1%
3	Appearance	Silvery white and odourless powder
4	Particle Size (µm)	20–100 µm (typical); common laboratory grade: 45–75 µm
5	Density (g/cm^{3})	2.7
6	Boiling Point (^{o}C)	2467
7	Melting Point (^{o}C)	660.1
8	Molecular Weight (kg/mol)	0.02698 kg/mol (26.98 g/mol)
9	Specific Heat@25^{0}C (Cal/kg^{o}C)	0.215
10	Thermal Conductivity @20^{o}C (W/m.k)	237
11	Co-efficient of Expansion@20-100 deg.C	23.1 × 10^{-6} /°C
12	Modulus of Elasticity (N/m^{2})	69
13	Specific gravity	2.6989
14	Crystallography	Cubic structure, face centered

Table 3: Properties of carbon black powder

S/N	Properties	Description
1	Surface Area (m^{2}/g)	7-11
2	Particle size	240-320nm
3	Morphology (ml/g) DBP	32- 47 ml/100 g DBP
4	Shape	Spheroidal, Ellipsoidal, Linear and Branch
5	Moisture Content	Moisture Content (as supplied) ≤ 1.0 wt.% Typical Range 0.2–0.8 wt.% Maximum (ASTM grade specification) ≤ 1.5 wt.%

Received: 22/06/2026; Revised: 04/07/2026; Accepted: 08/07/2026; Published: 11/07/2026

S/N	Properties	Description
6	Carbon black grade/type	Pyro black

2.1 Material Selection

The materials used for the design and fabrication of the injection moulding machine were based on availability of materials, ease of fabrication, serviceability, strength and cost. The key materials used are mild steel and cast iron. Due to its ability to resist corrosion, mild steel was used to fabricate the barrel assembly, shaft, nozzle, discharge runner, frame etc, while the cast iron was used to fabricate the heavy hex flange screw, and all screws. To minimize the effect of corrosion, the mild steel was painted. The following materials were obtained for the construction of the injection moulding machine: 2" Angle iron for frame, Ø71, 10mmx300lg for flange and nozzle holder, 500x500x10mm plate for Barrel, 1.2x1.2x1.2mm Ms Plate for flight and hopper, Ø30, 10mmx500lg (C4) for main shaft, 1.2x1.2x2mm Ms Plate, 250x4x1500mm Channel for support, 300x300x5mm plate for support and hanger, Harden high carbon Steel for nozzle, Belt type heating element, M8 Bolt and nut, Electrode, Cutting disc. Table 4, presents the justification for selection of the materials

Table 4: Material Selection and Justification for Injection Moulding Machine Components

S/N	Component/Material	Specification	Brief Justification for Selection
1	Frame	2" Angle Iron	Selected for its high structural strength, rigidity, good load-bearing capacity, ease of fabrication and welding, and ability to withstand vibration and operational stresses during moulding operations. It is also economical and readily available.
2	Flange and Nozzle Holder	Ø71 mm × 10 mm × 300 mm Mild Steel	Chosen because of its adequate tensile strength, machinability, and ability to withstand moderate thermal and mechanical stresses. Its good weldability facilitates assembly and maintenance.
3	Barrel	500 × 500 × 10 mm Steel Plate	Selected due to its high mechanical strength and heat resistance, enabling it to withstand the internal pressure and elevated temperatures generated during the melting and extrusion of plastic materials.
4	Flight and Hopper	1.2 × 1.2 × 1.2 mm Mild Steel Plate	Mild steel provides sufficient toughness, formability, and corrosion resistance for handling plastic granules. It is easy to fabricate into the required screw flight and hopper geometry and is cost-effective.
5	Main Shaft	Ø30 mm × 10 mm × 500 mm Carbon Steel (C4)	Chosen because of its high torsional strength, hardness, fatigue resistance, and ability to transmit rotational power effectively without excessive deformation or failure during operation.
6	Support Channel	250 × 4 × 1500 mm Channel Section	The channel section offers excellent bending strength, rigidity, and load distribution capabilities, thereby providing adequate support for the machine components and reducing structural deflection.
7	Support and Hanger	300 × 300 × 5 mm Steel Plate	Selected for its high compressive strength and rigidity, enabling it to support the weight of the barrel, motor, and heating components while maintaining machine stability.
8	Nozzle	Hardened High Carbon Steel	Chosen because of its excellent hardness, wear resistance, high-temperature strength, and resistance to abrasion and deformation caused by continuous flow of molten plastic under pressure.
9	Heating Element	Belt-Type Heating Element	Selected because it provides uniform and efficient circumferential heating of the barrel, possesses good thermal efficiency, rapid heating capability, ease of installation, and accurate temperature control required for plastic melting.
10	Fasteners	M8 Bolts and Nuts	Chosen for their adequate tensile strength, ease of assembly and disassembly, and ability to provide

Received: 22/06/2026; Revised: 04/07/2026; Accepted: 08/07/2026; Published: 11/07/2026

S/N	Component/Material	Specification	Brief Justification for Selection
			secure fastening of machine components during maintenance and operation.
11	Welding Material	Electrodes	Selected because they produce strong, reliable weld joints with good penetration and mechanical integrity necessary for fabricating the machine frame and structural components.
12	Cutting Tool	Cutting Disc	Chosen for its ability to provide accurate, clean, and efficient cutting of metallic materials during fabrication, thereby improving dimensional accuracy and reducing fabrication time.

2.2 Design Consideration and Assumptions

Barrel

In designing the barrel of the injection moulding machine, a single-stage plasticizing system was adopted, whereby plastic melting and injection occur simultaneously as the screw rotates, ensuring melt homogeneity. The barrel capacity was determined by the maximum volume of the plastic component to be produced, with dimensions selected to utilise 40–70% of the barrel capacity, facilitating efficient material flow and appropriate hopper positioning. The design was based on producing one sample per operation, using the bending test specimen with the largest volume of 37,200 mm³ as the basis for determining the barrel's internal volume. The principal design parameters considered were the internal diameter, length and wall thickness of the barrel, while the injection screw root diameter was selected as 260 mm based on material availability and the design recommendations.

For specimen volume, V_s a utilization factor U_f= 60%, and accounting for material losses such as sprues, runners and gates in the mould, the required barrel capacity, Vc, is given by Equation 1:

$$V_c = \frac{V_s}{U_f} \tag{1}$$

The volume of the cylinder technically referred to as the barrel is given by Equation 2:

$$V_c = \pi r_i^2 L \tag{2}$$

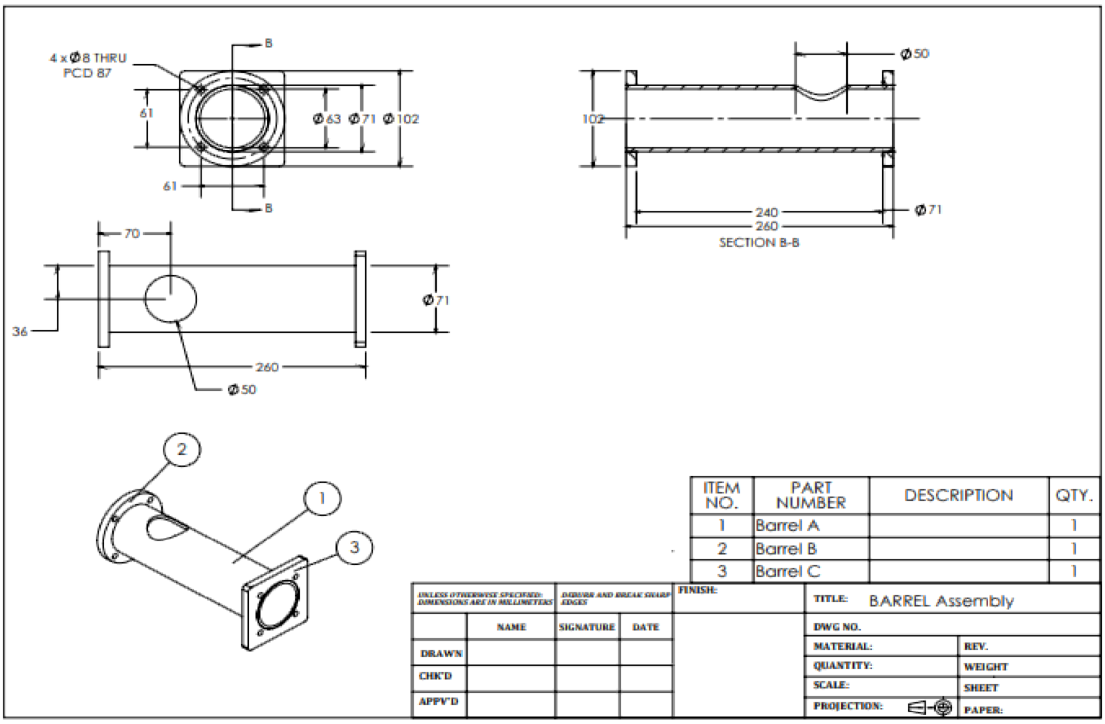

Figure 1: Diagram of the Barrel

Received: 22/06/2026; Revised: 04/07/2026; Accepted: 08/07/2026; Published: 11/07/2026

The barrel volume was determined using the required specimen volume and a pre-selected hollow mild steel barrel with an internal diameter of 71 mm. The calculated barrel length was 260 mm, giving an L/D ratio of 6:1. The fabricated barrel had an external diameter of 102 mm and a wall thickness of 6 mm, which was sufficient to achieve the desired heating temperature within 30 minutes while ensuring efficient heat transfer from the band heaters. The design of the barrel is presented in the Figure 1.

Screw Shaft

The injection screw was fabricated from mild steel pipes to perform four essential functions: conveying, melting, compressing, and injecting plastic into the mould. Based on the barrel design, a minimum L/D ratio of 6:1 and a compression ratio of 1.5:1 was adopted, although this was below the recommended 3:1 due to manufacturing limitations. The developed square-pitch screw had an outer diameter of 25 mm, inner diameter of 6 mm, flank of 20 mm, and helix angle of 20°. The design of the screw shaft is presented in Figure 2.

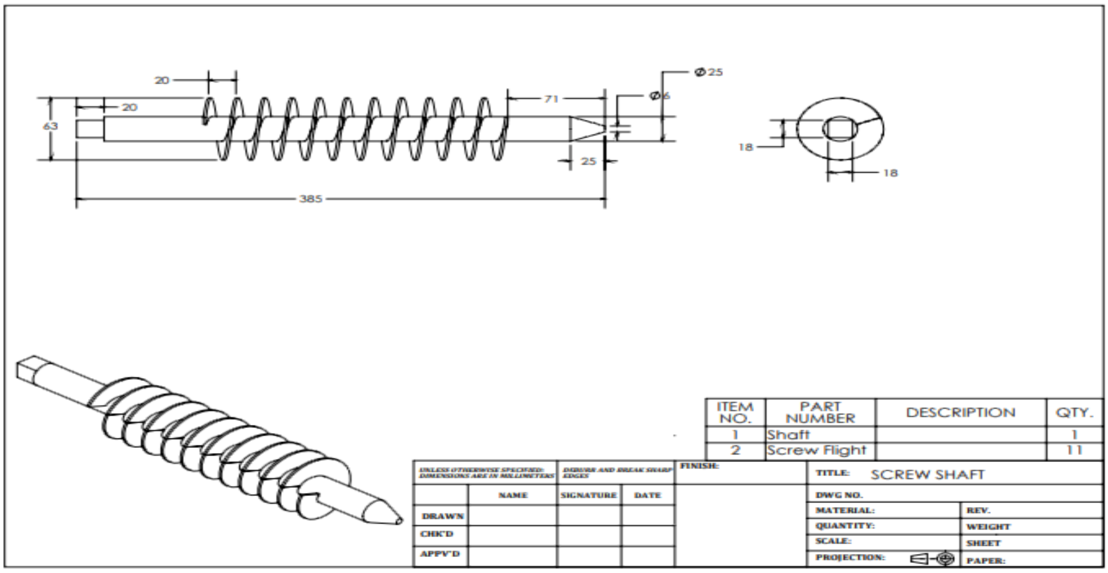

Figure 2: Diagram of the screw shaft

Nozzle

An open-channel, short nozzle was selected because it minimizes pressure loss, reduces shear heating, and prevents clogging during plastic processing. Due to size, location and cost constraints, a separate heater and thermocouple were not incorporated. Consequently, a 90 mm long, 10 mm internal diameter mild steel nozzle was fabricated as a practical compromise. Figure 3 presents the nozzle.

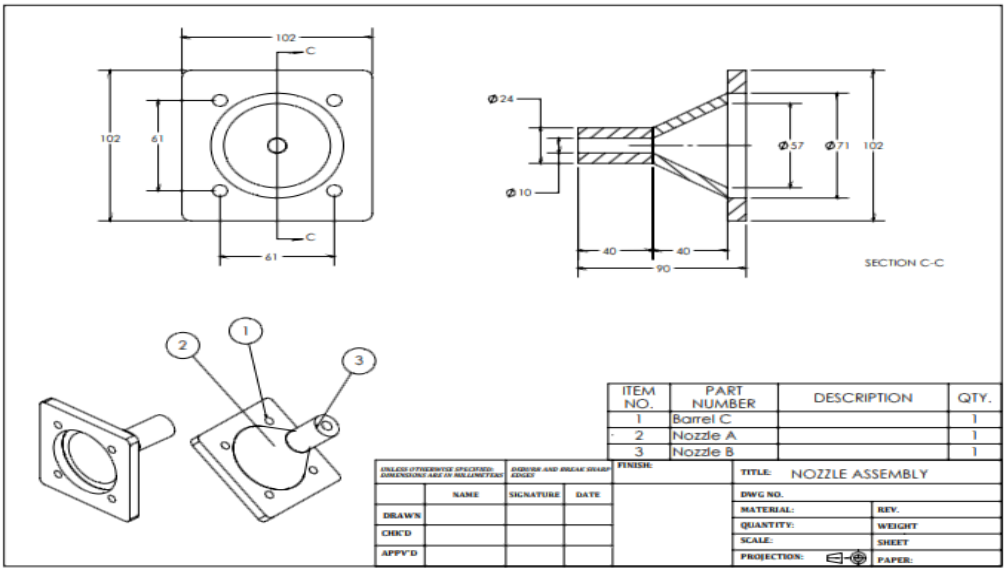

Figure 3: Diagram of the Nozzle

Received: 22/06/2026; Revised: 04/07/2026; Accepted: 08/07/2026; Published: 11/07/2026

Hopper

The hopper loads raw plastic to the heating chamber within the barrel. In order to utilize a large section of the barrel (40-70%), the location of the hopper is important. Therefore 18 the hopper was placed as close as possible to the inlet end of the barrel, and this allowed room (up to 70% of the barrel) for heating of the plastic. The Figure 4, presents the hopper.

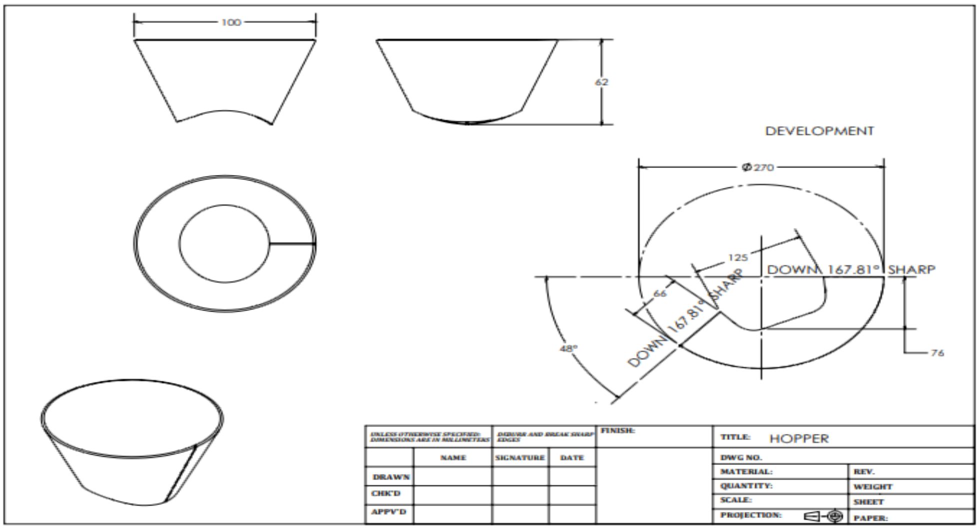

Figure 4: Diagram of the Hopper

Frame

The frame is the support of the injection moulding machine. It is made of angle bar which is strong enough to carry the weight of the machine, the frame also supports the electric motor mount the angle bar is sturdy therefore it allows for steady placement and would not move when grinding is taking place. Figure 5, presents the Frame.

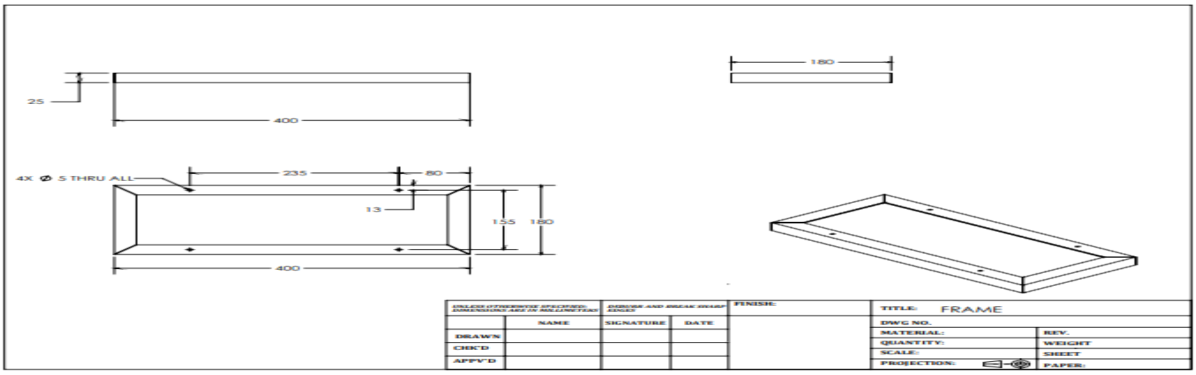

Figure 5: Diagram of the Frame

2.3 Design Calculations

Design of shaft

Generally, our hand can lift 25kg =250N

Now,

$$\tau = \frac{16T}{\pi d^3} \quad (3)$$

$$\therefore T = \frac{\pi \tau d^3}{16} \quad (4)$$

$$\therefore \text{ Force } \times \text{ distance } = \frac{\pi \tau d^3}{16} \quad (5)$$

$$\therefore 355 \times 355 = \frac{\pi \times 41 \times d^3}{16}$$

$$\therefore d = 25mm$$

So, the diameter of shaft is 25mm

Design of gear

Now, torque is given by

$$T = F_t \times d \quad (6)$$

Here, we assume V =8 m/sec (for ordinary cut gears)

$$P = \frac{F_t \times V}{1000} \quad (7)$$

$$P = \frac{355 \times 8}{1000} \quad (8)$$

P = 2.84k_w

Power = 2.84k_w

By using Lewis equation

$$W_T = \sigma_d \times C_v \times b \times Y \times m \quad (9)$$

σ_d = 47.1MN/mm^2

Where:

b= face width of gear

Y=form factor = π×y

y=0.154-0.912/z (for 20° involutes system)

y=0.0628

So, Y=0.198

For, cast iron grade 20;

$$C_v = \frac{3.05}{3.05 + V} \quad (10)$$

$$C_v = 0.27$$

Take, V=8 m/sec, b= 10m

$$W_t = \frac{P}{V}$$

$$\therefore 47.1 \times 10^6 \times 0.27 \times 10m \times m \times 0.198 = \frac{2 \times 10^3}{8}$$

$$\therefore m = 3.12$$

For standard value of module take m=3'

Data of gear

Pitch circle diameter=3×10=30mm

$$Pitch = \pi \times \frac{D}{Z} = 10mm \quad (11)$$

Addendum=m=3mm

Dedendum=1.25m=3.75mm

Clearance= 0.25m=0.75mm

Working depth= 2m=6mm

Whole depth= 2.25m=6.75mm

Tooth thickness= 1.57m=4.71mm

Fillet radius= 0.4m=1.2mm

Design of plunger

One rotation of handle=one rotation of gear=no. of teeth × pitch =10×10

Effective Length =100 mm

Diameter of the plunger: Volume of plunger=volume of barrel

$$\frac{\pi}{4} d_p^2 \times l_e = \frac{m}{p} \quad (12)$$

$$\therefore d_p = \sqrt{\frac{4m}{\pi p l_e}} \quad (13)$$

$$\therefore d_p = \sqrt{\frac{4 \times 35}{\pi \times 0.92 \times 100}}$$

$$\therefore d_p = 21mm$$

So, the diameter of the plunger is 21 mm

Total length = 4 × Effective Length = 4 × 100 = 400 mm

Received: 22/06/2026; Revised: 04/07/2026; Accepted: 08/07/2026; Published: 11/07/2026

Design of barrel
Diameter of barrel = Diameter. Of plunger + 1mm clearance = 21 + 1 = 22 mm
External diameter of barrel = Diameter of barrel + 2×thickness of barrel = 22 + 2(7) = 36 mm
Internal diameter of barrel = diameter. Of plunger + clearance = 21 + 1 = 22 mm

2.4 Fabrication and Assembly of the Machine Component

Step 1: Material Selection and Procurement

The required materials, including angle irons, mild steel plates, channels, carbon steel shafts, hardened high-carbon steel, bolts and nuts, and heating elements, were sourced locally based on their mechanical strength, thermal properties, availability, and cost-effectiveness.

Step 2: Design and Measurement

Detailed engineering drawings and dimensions of the machine components, such as the frame, barrel, screw, nozzle, hopper, and support structures, were prepared. The materials were marked out according to the specified dimensions.

Step 3: Cutting of Materials

The selected materials were cut to the required sizes using an industrial cutter and cutting discs. The angle irons, plates, channels, and shafts were cut according to the design specifications.

Step 4: Fabrication of the Main Frame

The 2-inch angle irons were cut and welded together to form the machine frame. The frame was fabricated to provide adequate rigidity, load-bearing capacity, and stability during machine operation.

Step 5: Fabrication of the Barrel

The mild steel barrel was fabricated with an internal diameter of 71 mm, a length of 260 mm, and a wall thickness of 6 mm. The barrel was machined and prepared to accommodate the screw assembly and heating elements.

Step 6: Fabrication of the Injection Screw

A square-pitch screw was fabricated from mild steel pipes based on the designed dimensions. The screw flights were formed and welded onto the shaft to facilitate conveying, mixing, compression, and injection of molten plastic.

Step 7: Fabrication of the Nozzle

A short open-channel nozzle with a length of 90 mm and an internal diameter of 10 mm was fabricated from hardened high-carbon steel to provide unrestricted flow of molten plastic and reduce clogging.

Step 8: Fabrication of the Hopper

The hopper was fabricated from 1.2 mm mild steel plate through cutting, bending, and welding operations. The hopper was designed to allow continuous and efficient feeding of plastic granules into the barrel.

Step 9: Fabrication of Support Structures

Supporting plates, channels, and hangers were fabricated from mild steel plates and channels. Holes for bolts and assembly were drilled using a hand drill and puncher.

Step 10: Surface Finishing

All welded joints and rough surfaces were smoothened using a grinder to improve appearance, eliminate sharp edges, and enhance operational safety.

Procedural Steps for Assembly of the Injection Moulding Machine

Step 11: Installation of the Main Frame

The fabricated frame was placed on a level surface and checked for proper alignment and structural stability.

Step 12: Installation of Supporting Plates

The supporting plates were positioned and bolted onto the frame using tie bars and bolts to provide support for the barrel and other machine components.

Step 13: Mounting of the Barrel

The fabricated barrel was aligned and bolted onto the supporting plates to ensure proper positioning and stability.

Step 14: Installation of the Screw and Main Shaft Assembly
The injection screw and main shaft assembly were inserted through the supporting plates and positioned inside the barrel. Proper alignment was ensured to facilitate smooth rotational motion.

Step 15: Installation of the Drive Unit
The drive system comprising the electric motor, reduction gearbox, and spur gears was mounted and coupled to the screw shaft to provide the required rotational speed and torque.

Step 16: Installation of the Heating System
The belt-type heating elements were fixed around the barrel and connected to the temperature control unit to provide uniform heating for plastic melting.

Step 17: Installation of the Locking Mechanism
The handle and locking device were installed through the supporting plate and connected to the platen assembly to facilitate mould opening and closing operations.

Step 18: Installation of the Mould Assembly
The mould was positioned and securely fixed to the supporting plates and platen. Proper alignment was carried out to ensure efficient injection and easy removal of moulded products.

Step 19: Inspection and Testing
The assembled machine was inspected for alignment, mechanical integrity, electrical connections, and safety. Trial runs and performance tests were conducted to verify proper operation of the heating, injection, and moulding systems.

3.0 Performance Evaluation

The performance evaluation of the injection moulding machine was conducted to determine the effects of injection pressure, injection time and injection temperature on cavity pressure during the moulding cycle. The experiment involved low-density polyethylene (LDPE) reinforced with aluminium powder and carbon black, using a rectangular mould cavity of uniform thickness. The composite materials were processed at an injection temperature of 250°C and 200 ^{o}C, respectively. The temperature was chosen to ensure complete melting and homogeneous dispersion of the reinforcing particles (aluminium and carbon black), the exposure time of the melt at this temperature was short, thereby minimizing thermal degradation, no visible degradation (burning, discoloration, excessive fumes, or brittleness) was observed during processing and the selected temperature produced acceptable mould cavity pressure and satisfactory product quality. The machine had a maximum injection pressure of 2,500 bar, a cylinder diameter of 22 mm, and a maximum product capacity of 200 g. During operation, polymer materials were fed through the hopper into the plasticization cylinder, melted, and injected into the mould cavity through the runner and gate, after which the moulded products were cooled by air and ejected. For each experimental case, process parameters were adjusted until steady-state conditions were attained, temperatures were monitored to prevent excessive cavity pressure, and moulding cycles were conducted while ensuring parameter stability throughout the experiment. The parameters used in the experiment are presented in Table 5.

Table 5: Process parameters used

Process parameters	**Value**
Cooling air temperature	25 ℃
Packing time	35 sec
Packing temperature (LDPE/aluminium powder)	50 ℃
Packing temperature (LDPE/carbon black)	45 ℃
Injection pressure	60 MPa
Injection time	1.535 sec
Ejection time	7.65
Injection speed	30 mm/s
Cooling time	145
Rotation velocity	100 rpm

Design of Experiment

The Box–Behnken Design (BBD) is ideal because: It requires fewer experimental runs than a full factorial design. It efficiently estimates quadratic effects and interactions. It avoids extreme combinations of factor levels, which is advantageous when processing polymers near their degradation temperature. Fifteen experimental runs were carried out.

Factors and Levels

Factor	Symbol	Low (-1)	Centre (0)	High (+1)
Injection Pressure (bar)	A	800	1200	1600
Injection Time (s)	B	4	6	8
Injection Temperature (°C)	C	200	225	250

3.1 Results and Discussion

The results obtained from effect of injection pressure on mould cavity pressure of LDPE/Aluminum at 250℃ and LDPE/carbon black at 200℃.

Table 6: Injection pressure and mould cavity pressure of LDPE/aluminium at 250℃

Cavity pressure (MPa)	Injection pressure (MPa)
22	39
30	42
33	50
35	54
37	60
42	70

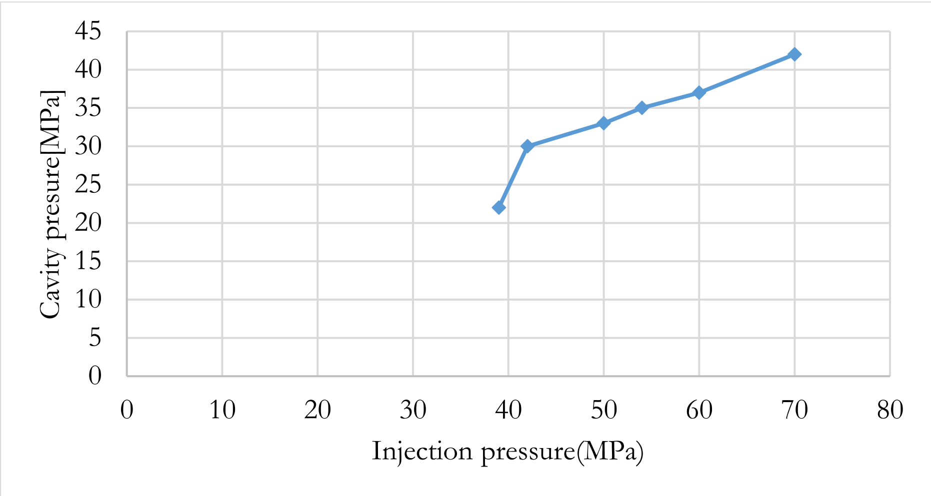

Figure 6: Cavity pressure (MPa) against injection pressure (MPa) at 250℃

Table 6 and Figure 6 indicate a direct relationship between injection pressure and mould cavity pressure. As the injection pressure increased from 39 MPa to 70 MPa, the mould cavity pressure correspondingly increased from 22 MPa to 42 MPa, demonstrating an approximately linear relationship. The increase in cavity pressure can be attributed to improved packing of the molten LDPE/aluminium composite inside the mould cavity [28]. Higher injection pressures increase the driving force required to overcome the viscosity of the polymer melt and ensure complete filling of the cavity [28]. This observation agrees with the findings of [29], who reported that cavity pressure is strongly dependent on injection pressure because pressure controls melt flow, material compaction and shrinkage behaviour. higher cavity pressure enhances packing density and compensates for volumetric shrinkage during cooling [30]. Consequently, moulded parts exhibit reduced warpage, lower sink marks and improved dimensional accuracy [30]. Studies by Baum et al. [31] demonstrated that increased packing pressure significantly improves dimensional consistency in thermoplastic injection moulding [31]. The incorporation of aluminium particles increases thermal conductivity and stiffness of the LDPE matrix. Higher cavity pressures improve particle dispersion and reduce internal voids, leading to better tensile and flexural properties [30-31]. Similar observations were reported by researchers investigating metal-particle-reinforced thermoplastics, where

Received: 22/06/2026; Revised: 04/07/2026; Accepted: 08/07/2026; Published: 11/07/2026

increased packing pressure improved interfacial bonding and reduced porosity [32]. Adequate cavity pressure facilitates complete mould filling and replication of mould surfaces, producing smoother surfaces and minimizing weld lines and short shots. However, excessively high cavity pressure may generate flash formation and induce residual stresses. Therefore, the observed increase in cavity pressure up to 42 MPa suggests improved part consolidation and better overall product quality for LDPE/aluminium composites [33-34].

Table 7: Injection pressure and mould cavity pressure of LDPE/carbon black at 200℃

Cavity pressure (MPa)	Injection pressure (MPa)
20	39
29	42
32	50
33	55
34	65
37	70

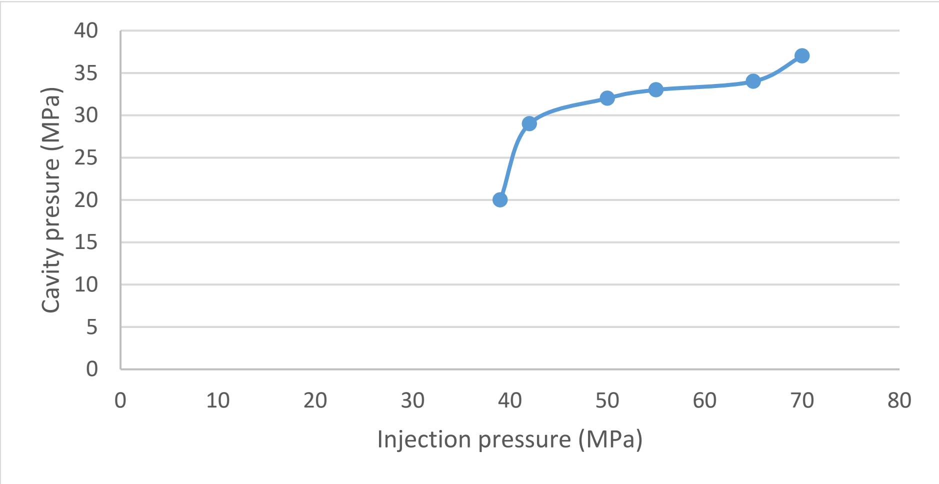

Figure 7: Cavity pressure (MPa) against injection pressure (MPa) at 200℃

Table 7 and Figure 7 also show a positive relationship between injection pressure and cavity pressure. As injection pressure increased from 39 MPa to 70 MPa, cavity pressure increased from 20 MPa to 37 MPa. The cavity pressures obtained for LDPE/carbon black were consistently lower than those observed for LDPE/aluminium at corresponding injection pressures. This behaviour may be attributed to differences in thermal conductivity, particle morphology and rheological characteristics of the carbon-black-filled composite. Carbon black particles increase melt viscosity and alter the flow characteristics of LDPE. According to [35] studies, fillers with high surface area can increase resistance to flow, resulting in lower pressure transmission within the mould cavity. Moderate cavity pressures reduce improve dimensional uniformity [36]. However, lower cavity pressures may cause incomplete packing and after cooling [37-39]. Results obtained from the effect of injection time on mould cavity pressure of LDPE/aluminium at 250℃ and LDPE/carbon black at 200℃.

Table 8: Injection time on mould cavity pressure of LDPE/aluminium at 250℃

Cavity pressure (MPa)	Injection time (MPa)
47	1.0
45	1.22
43	1.32
38	1.50
35	1.70
30	1.85

Received: 22/06/2026; Revised: 04/07/2026; Accepted: 08/07/2026; Published: 11/07/2026

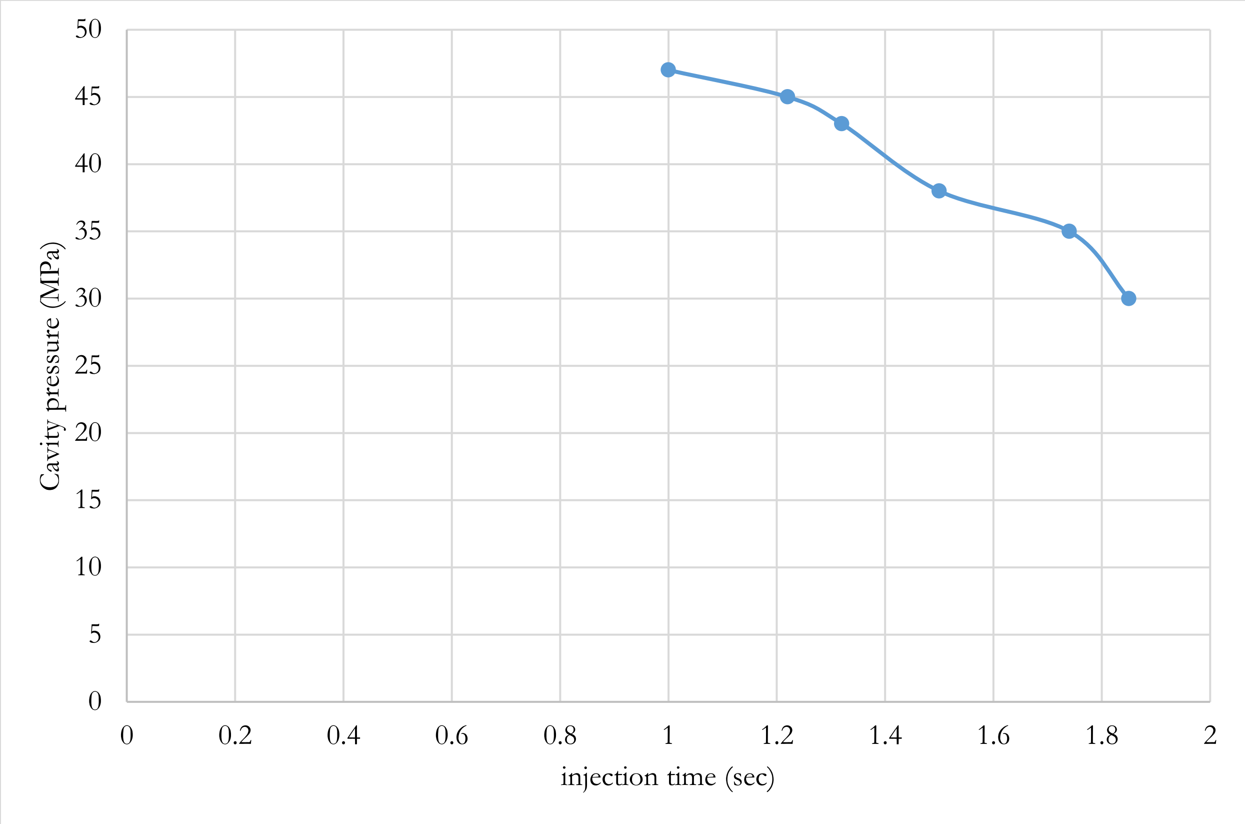

Figure 8: Cavity pressure (MPa) against injection time (sec) at 250℃

Table 8 and Figure 8 reveal an inverse relationship between injection time and cavity pressure. As injection time increased from 1.0 s to 1.85 s, cavity pressure decreased from 47 MPa to 30 MPa. This trend occurs because longer injection times imply lower filling rates and reduced pressure build-up inside the cavity. Polymer processing literature indicates that shorter filling times produce higher shear rates and greater cavity pressures, resulting in improved material compaction [40]. Higher cavity pressures obtained at shorter injection times reduce shrinkage and improve dimensional precision [41]. Longer injection times may permit premature cooling and incomplete packing, increasing the risk of warpage. Higher cavity pressures achieved at shorter injection times improve particle distribution and reduce porosity, thereby enhancing tensile strength and stiffness of LDPE/aluminium composites [41]. Short injection times improve surface replication and minimize sink marks [42]. However, excessively short times may generate burn marks and residual stresses. The optimum injection time appears to be within 1.0–1.3 s, where cavity pressure remained sufficiently high (43–47 MPa) to ensure good product quality.

Table 9: Injection time on mould cavity pressure LDPE/carbon black at 200℃

Cavity pressure (MPa)	**Injection time (sec)**
39	1.0
34	1.38
33	1.50
32	1.60
31	1.70
30	1.83

Received: 22/06/2026; Revised: 04/07/2026; Accepted: 08/07/2026; Published: 11/07/2026

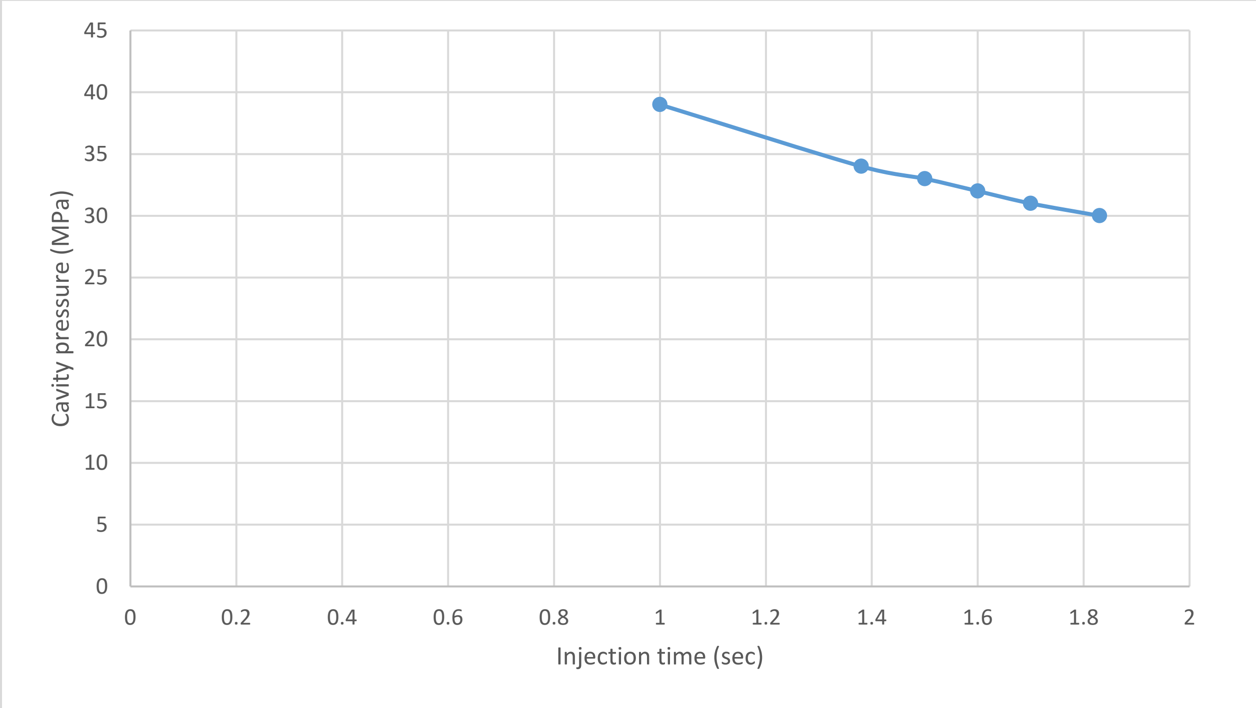

Figure 9: Cavity pressure (MPa) against injection time (sec) at 200℃

Table 9 and Figure 9 similarly demonstrate that increasing injection time from 1.0 s to 1.83 s caused cavity pressure to decrease from 39 MPa to 30 MPa. This finding is consistent with established injection moulding theory, which states that prolonged filling time reduces the rate of pressure transmission to the mould cavity because of increased heat loss and gradual solidification of the polymer melt [32]. Higher cavity pressures at shorter injection times improve packing efficiency [30]. The pressure-time relationship was similar for CB, but peak pressures were ~8 MPa lower than Al at 1.0 s. This suggests a higher flow resistance in the CB system

4.0 Conclusion

The study established that mould cavity pressure is a critical process parameter governing the quality of injection-moulded LDPE composites. Appropriate control of injection pressure and injection time is essential for achieving optimal cavity pressure, which in turn determines the dimensional accuracy of LDPE reinforced with aluminium and carbon black powders. The results further demonstrate that LDPE/aluminium composites exhibit better pressure response and potentially superior product quality compared with LDPE/carbon black composites under the investigated processing conditions.

References

[1] S. S. Shakurahmed, Design and Fabrication of Injection Moulding Machine for Small Scale Industries. Summary Report, Department of Mechanical Engineering, University of Pune, Pune, India, 2013.

[2] G. Singh, M. K. Pradhan, and A. Verma, "Effect of injection moulding process parameters on tensile strength using the Taguchi method," International Journal of Mechanical, Aerospace, Industrial, Mechatronic and Manufacturing Engineering, vol. 9, no. 10, pp. 1–6, 2015.

[3] S. H. Tang, Y. M. Kong, S. M. Sapuan, R. Samin, and S. Sulaiman, "Design and thermal analysis of plastic injection mould," Journal of Materials Processing Technology, vol. 171, no. 2, pp. 259–267, 2006.

[4] R. J. Crawford, Rubber and Plastic Engineering Design and Application. London, U.K.: Applied Science Publishers, 1987, p. 110.

[5] H. Hassan, N. Regnier, C. Le Bot, and G. Defaye, "3D study of cooling system effects on heat transfer during polymer injection molding," International Journal of Thermal Sciences, vol. 49, no. 1, pp. 161–169, 2010.

[6] A. T. Bozdana and O. Eyercıoglu, "Development of an expert system for the determination of injection moulding parameters of thermoplastic materials: EXPIMM," Journal of Materials Processing Technology, vol. 128, nos. 1–3, pp. 113–122, 2002.

[7] K. M. Tsai, C. Hsieh, and W. C. Lo, "A study of the effects of process parameters for injection molding on surface quality of optical lenses," Journal of Materials Processing Technology, vol. 209, no. 7, pp. 3469–3477, 2009.

Received: 22/06/2026; Revised: 04/07/2026; Accepted: 08/07/2026; Published: 11/07/2026

[8] H. Hassan, R. N. Nicolas, and G. Defaye, "3D study on the effect of process parameters on the cooling of polymers during injection molding," Journal of Applied Polymer Science, vol. 114, no. 5, pp. 2901–2914, 2009.

[9] T. D. Papathanasiou, "Flow-induced alignment in injection molding of fibre-reinforced polymer composites," in Flow-Induced Alignment in Composite Materials, Woodhead Publishing Series in Composites Science and Engineering, Cambridge, U.K.: Woodhead Publishing, 1997, ch. 4, pp. 112–163.

[10] H. Mensler, A Method for Determining the Flow Front Position and Velocity of a Polymer Melt in an Injection Moulding Process, Ph.D. dissertation, University of Gloucestershire, Cheltenham, U.K., 2022.

[11] P. H. P. M. da Silveira, M. D. N. da Conceição, D. N. de Pina, P. A. de Moraes Paes, S. N. Monteiro, N. D. L. C. O. Tapanes, et al., "Impact of different mineral reinforcements on HDPE composites: Effects of melt flow index and particle size on physical and mechanical properties," Polymers, vol. 16, no. 14, Art. no. 2063, 2024.

[12] C. Wu, F. Xu, H. Wang, H. Liu, F. Yan, and C. Ma, "Manufacturing technologies of polymer composites: A review," Polymers, vol. 15, no. 3, Art. no. 712, 2023.

[13] U. Siddique, "Effect of gating design on melt flow velocity in gravity sand casting using AM-enabled technology," 2025.

[14] G. Trotta, B. Stampone, and G. Tosello, "Performance characterisation of a micro-injection moulding machine and influence of operative conditions on the process simulation accuracy," Journal of Manufacturing Processes, vol. 172, pp. 924–938, 2026.

[15] S. Dayanand and S. B. Boppana, "Manufacturing of particulate and fiber reinforced composites: A review," in Structural Composite Materials: Fabrication, Properties, Applications and Challenges, pp. 119–142, 2023.

[16] O. Okolie, Influence of Process Parameters and Manufacturing Defects on the Properties of Thermoplastic Composite Pipes, Ph.D. dissertation, 2024.

[17] V. Momeni, M. Hufnagl, Z. Shahroodi, J. Gonzalez-Gutierrez, S. Schuschnigg, C. Kukla, and C. Holzer, "Research progress on low-pressure powder injection molding," Materials, vol. 16, no. 1, Art. no. 379, 2023.

[18] S. Zhou and A. N. Hrymak, "Injection molding of polymers and polymer composites," Polymers, vol. 16, no. 13, Art. no. 1796, 2024.

[19] Z. Shan, H. Li, X. Qin, and W. Wu, "The filling behavior characteristics, performance and consistency of LDPE in the microscale convergent cavity during the ultrasonic plasticizing micro-injection molding process," Journal of Manufacturing Processes, vol. 155, pp. 242–260, 2025.

[20] C. W. Su, W. J. Su, F. J. Cheng, G. Y. Liou, S. J. Hwang, H. S. Peng, and H. Y. Chu, "Optimization of process parameters and adaptive quality monitoring for injection molding of materials with different viscosities," Polymer Testing, vol. 109, Art. no. 107526, 2022.

[21] T. Wang, T. Zheng, F. Zeng, and L. Guo, "Effect of compaction rate during cyclic compaction on the compaction response of vacuum infusion consumables," Thin-Walled Structures, vol. 206, Art. no. 114173, 2025.

[22] M. Sabbrojjaman, A. Manalo, W. Ferdous, and O. Alajarmeh, "Mechanical and durability characteristics of particulate-filled recycled thermoplastic composites (RTCs): A comprehensive review," Polymers, vol. 17, no. 23, Art. no. 3161, 2025.

[23] J. G. Zhang, M. J. Edirisinghe, and R. G. Evans, "The control of sprue solidification time in ceramic injection moulding," Journal of Materials Science, vol. 24, no. 3, pp. 840–848, 1989.

[24] W.-C. J. Wei, R.-Y. Wang, and S.-J. Ho, "Effects of pressure parameters on alumina produced by powder injection moulding," Journal of the European Ceramic Society, vol. 20, no. 9, pp. 1301–1310, 2000.

[25] R. Pareek and J. Bhamniya, "Optimization of injection moulding process using Taguchi and ANOVA," Journal of Scientific and Engineering Research, vol. 4, no. 1, pp. 1–6, 2013.

[26] H. Hassan, "An experimental investigation of the effect of injection moulding parameters on cavity pressure and product weight," The International Journal of Advanced Manufacturing Technology, vol. 67, nos. 1–4, pp. 675–686, 2013.

[27] Y. Wu, Y. Gong, K. J. Cha, and J. M. Park, "Effect of microstructures on the shrinkage of injection moulded products," Journal of Mechanical Science and Technology, vol. 33, no. 3, pp. 1357–1363, 2019.

[28] E. I. Bello, T. I. Ogedengbe, L. Lajide, and I. A. Daniyan, "Optimization of process parameters for biodiesel production using response surface methodology," American Journal of Energy Engineering, vol. 4, no. 2, pp. 8–16, 2016.

[29] N. Kaliappan, P. Sivaraman, K. S. Raghul, H. Alemayehu, K. Mohan, and M. K. Prabhu, "Moldflow-based simulation of flow dynamics in nano-filled polymer injection molding: A comprehensive rheological and thermal analysis," Scientific Reports, vol. 16, 2026.

[30] K. F. Liew, H. S. Peng, P. W. Huang, and W. J. Su, "Injection barrel/nozzle/mold-cavity scientific real-time sensing and molding quality monitoring for different polymer-material processes," Sensors, vol. 22, no. 13, Art. no. 4792, 2022.

Received: 22/06/2026; Revised: 04/07/2026; Accepted: 08/07/2026; Published: 11/07/2026

[31] M. Baum, D. Anders, and T. Reinicke, "Approaches for numerical modeling and simulation of the filling phase in injection molding: A review," Polymers, vol. 15, no. 21, Art. no. 4220, 2023.

[32] S. C. Chen, B. L. Tsai, C. C. Hsieh, N. T. Cheng, E. N. Shen, and C. T. Feng, "Prediction of part shrinkage for injection molded crystalline polymer via cavity pressure and melt temperature monitoring," Applied Sciences, vol. 13, no. 17, Art. no. 9884, 2023.

[33] C. Araújo, D. Pereira, D. Dias, R. Marques, and S. Cruz, "In-cavity pressure measurements for failure diagnosis in the injection moulding process and correlation with numerical simulation," The International Journal of Advanced Manufacturing Technology, vol. 126, nos. 1–2, pp. 291–300, 2023.

[34] K. Wilczyński, K. J. Wilczyński, and K. Buziak, "Modeling and experimental studies on polymer melting and flow in injection molding," Polymers, vol. 14, no. 10, Art. no. 2106, 2022.

[35] J. Li, H. Ma, W. Liu, S. Jiang, and B. Pan, "Effects of cavity thickness and mold surface roughness on the polymer flow during micro injection molding," Polymers, vol. 15, no. 2, Art. no. 326, 2023.

[36] T. M. T. Uyen, P. S. Minh, and B. C. Thanh, "Application of cooling layer and reduced thickness between coolant and cavity for mold temperature control and improved filling ability of thin-wall injection molded products," Polymers, vol. 17, no. 19, Art. no. 2658, 2025.

[37] S. Zhao, D. Tang, Y. Fang, X. Hao, Y. Liu, J. Liu, H. Zhao, C. Sun, C. Hua, A. K. Schlarb, and L. Lin, "Enhanced wear resistance of sustainable tire materials with plasma-modified pyrolysis carbon black," Carbon, vol. 213, Art. no. 118201, 2023.

[38] X. Wang, S. Cheng, Z. Hao, H. Duan, B. Li, G. Zhao, Y. Liu, and X. Duan, "Improving the mechanical properties and wear resistance of rubber/graphene composites through surface modification of carbon black," Polymer Composites, vol. 47, no. 5, pp. 4386–4397, 2026.

[39] M. H. K. Tareen, F. Hussain, Z. Zubair, S. Aslam, T. Saleem, M. Awais, A. Farooq, and I. Goda, "Effects of carbon black on epoxidized natural rubber composites: Rheological, abrasion, and mechanical study," Journal of Composite Materials, vol. 56, no. 29, pp. 4473–4485, 2022.

[40] Y. Xu, S. Wu, Z. Chen, X. Wu, J. Zhang, and B. Xiao, "Study on compaction characteristics and mechanical model of dry crushing filling material under lateral confinement conditions," Scientific Reports, vol. 14, no. 1, Art. no. 14910, 2024.

[41] A. A. Nasr, B. Wang, S. Chen, and F. Jin, "Monitoring the flow patterns of high-performance self-compacting concrete in the voids of sloped rock-filled concrete structures," Ain Shams Engineering Journal, vol. 16, no. 3, Art. no. 103313, 2025.

[42] B. Kohlhaas and J. H. Finke, "Investigation of differences in mechanisms of die filling between a compaction simulator and a rotary press," International Journal of Pharmaceutics: X, vol. 8, Art. no. 100405, 2025.

Received: 22/06/2026; Revised: 04/07/2026; Accepted: 08/07/2026; Published: 11/07/2026